

DTIC FILE COPY

MASTER COPY

FOR REPRODUCTION PURPOSES

2

AD-A199 863

REPORT DOCUMENTATION PAGE

2a SECURITY CLASSIFICATION AUTHORITY		1b RESTRICTIVE MARKINGS	
2b DECLASSIFICATION/DOWNGRADING SCHEDULE		3 DISTRIBUTION AVAILABILITY OF REPORT Approved for public release; distribution unlimited.	
4 PERFORMING ORGANIZATION REPORT NUMBER(S)		5 MONITORING ORGANIZATION REPORT NUMBER(S) ARO 25532.1-EL-SBI	
6a NAME OF PERFORMING ORGANIZATION KOPPIN Corp.	6b OFFICE SYMBOL (if applicable)	7a NAME OF MONITORING ORGANIZATION U. S. Army Research Office	
6c ADDRESS (City, State, and ZIP Code) Taunton, MA 02780		7b ADDRESS (City, State, and ZIP Code) P. O. Box 12211 Research Triangle Park, NC 27709-2211	
8a NAME OF FUNDING/SPONSORING ORGANIZATION U. S. Army Research Office	8b OFFICE SYMBOL (if applicable)	9 PROCUREMENT INSTRUMENT IDENTIFICATION NUMBER DAAL03-87-C-0025	
8c ADDRESS (City, State, and ZIP Code) P. O. Box 12211 Research Triangle Park, NC 27709-2211		10 SOURCE OF FUNDING NUMBERS	
		PROGRAM ELEMENT NO	PROJECT NO
		TASK NO	WORK UNIT ACCESSION NO
11 TITLE (Include Security Classification) Dual-Susceptor OMCVD for Production of Heterostructure Materials			
12 PERSONAL AUTHOR(S) Roand P. Gale			
13a TYPE OF REPORT Final	13b TIME COVERED FROM 10.1.87 TO 3/31/88	14 DATE OF REPORT (Year, Month, Day) April 1988	15 PAGE COUNT 30
16 SUPPLEMENTARY NOTATION The view, opinions and/or findings contained in this report are those of the author(s) and should not be construed as an official Department of the Army position, policy, or decision, unless so designated by other documentation.			
17 COSATI CODES		18 SUBJECT TERMS (Continue on reverse if necessary and identify by block number)	
FIELD	GROUP	SUB-GROUP	
19 ABSTRACT (Continue on reverse if necessary and identify by block number)			
<div style="text-align: right;"> <p><b>DTIC ELECTE</b></p> <p><b>S</b> <b>D</b></p> <p>OCT 20 1988</p> <p>E</p> </div>			
20 DISTRIBUTION AVAILABILITY OF ABSTRACT <input type="checkbox"/> UNCLASSIFIED/UNLIMITED <input type="checkbox"/> SAME AS RPT <input type="checkbox"/> DTIC USERS		21 ABSTRACT SECURITY CLASSIFICATION Unclassified	
22a NAME OF RESPONSIBLE INDIVIDUAL		22b TELEPHONE (Include Area Code)	22c OFFICE SYMBOL

# DUAL-SUSCEPTOR OMCVD FOR PRODUCTION OF HETEROSTRUCTURE MATERIALS

## PHASE I PROJECT SUMMARY

A new generation of electronic and photonic devices requires advanced heterostructures. The large-scale production of high electron mobility transistors and quantum-well optoelectronic devices requires the deposition of atomically abrupt layers of gallium arsenide and related III-V materials uniformly over large areas. This Phase SBIR project addresses the application of organometallic chemical vapor deposition (OMCVD) to this purpose. Specifically, we have developed a new type of OMCVD reaction chamber that offers superior uniformity and abruptness, and that additionally yields high material utilization and reduced growth temperature.

In brief, the innovation described here comprises dual rotating vertical surfaces onto which GaAs substrate wafers are mounted. These surfaces (susceptors) are heated to the crystal growth temperature, so that when the chemical vapor that contains the Ga and As passes between the rotating susceptors, a thin film with an atomically abrupt interface is deposited. The principles of the operation of this reactor were demonstrated. In accordance with the Phase I plan, we investigated the effect of growth conditions on layer uniformity, demonstrated the deposition of thin, abrupt layers, and identified critical growth parameters and operation issues necessary for reactor scale up in Phase II. We completed each of these tasks and demonstrated feasibility of the reactor design in Phase I.

A production reactor using this design will be capable of reproducibly depositing large areas of uniform layers with extremely abrupt interfaces. Applications for these wafers range from high speed HEMT structures for fifth generation supercomputers to quantum and multiquantum-well structures for optical communications.

Accession For	
NTIS GRA&I	<input checked="" type="checkbox"/>
DTIC TAB	<input type="checkbox"/>
Unannounced	<input type="checkbox"/>
Justification	
By	
Distribution/	
Availability Codes	
Dist	Avail and/or Special
A-1	



88 10 19 004

(Page 1)

This SBIR data is furnished with SBIR rights under Contract No. DAAL03-87-C-0025. For a period of 2 years after acceptance of all items to be delivered under this contract the Government agrees to use this data for Government purposes only, and it shall not be disclosed outside the Government (including disclosure for procurement purposes) during such period with permission of the Contractor, except that, subject to the foregoing use and disclosure prohibitions, such data may be disclosed for use by support contractors. After the aforesaid 2-year period the Government has a royalty-free license to use, and to authorize others to use on its behalf, this data for Government purposes. This restriction does not limit the Government's right to use information contained in the data if it is obtained from another source without restriction. The data subject to this restriction is contained in pages   \*\*   of this report.

\*\* Pages 2, 3, 4, 5, 6, 7, 12, 13, 18, 19, 20, 21, 22, 23, 24,  
25, 26, 27

DUAL-SUSCEPTOR OMCVD FOR PRODUCTION OF  
HETEROSTRUCTURE MATERIALS

PHASE 1 SBIR CONTRACT FINAL REPORT

1 OCTOBER 1987 - 31 MARCH 1988

Ronald P. Gale  
Kopin Corporation  
Taunton, MA 02780

April 1988

Prepared under SBIR Contract No. DAAL03-87-C-0025  
Project No. P-25532-EL-S  
U.S. Army Research Office  
Research Triangle Park, NC

## TABLE OF CONTENTS

	<u>PAGE</u>
List of Figures	v
1. Introduction	1
2. Objectives of Phase I	4
3. Summary of Research and Findings	6
4. Review of Objectives	27
5. Analysis of Feasibility	28
6. Summary	29
References	30

## LIST OF FIGURES

- Figure 1-1 Cross sectional schematic of the dual-susceptor reactor
- Figure 1-2 Prototype dual-susceptor reactor
- Figure 3-1 Growth rate plotted as a function of vertical position along a 2" wafer for deposition at three different gas flow rates.
- Figure 3-2 Average growth rate
- Figure 3-3 Growth rate uniformity along 2" wafers deposited at a temperature of 640°C and pressures of 30, 120, and 240 torr.
- Figure 3-4 Growth rate uniformity along 2" wafers deposited at a temperature of 580°C and 152, 228, 304, and 380 torr.
- Figure 3-5 Gas inlet configuration in the prototype reactor.
- Figure 3-6 Lateral growth rate uniformity of a wafer deposited at 640°C and 120 torr.
- Figure 3-7 Cross sectional transmission electron micrograph of a GaAs/AlAs heterostructure.
- Figure 3-8 The deposition run corresponding to the curve for 228 torr pressure, plotted along with the experimental curve.
- Figure 3-9 Model output of the prototype dual-susceptor reactor showing TMGa mass fraction in cross section for the simulation of Figure 3-8.
- Figure 3-10 Model output of the prototype dual-susceptor reactors showing temperature in cross section for the simulation of Figure 3-8.
- Figure 3-11 Model output of the prototype dual-susceptor reactor showing vertical velocity of the gas in cross section for the simulation of Figure 3-8.
- Figure 3-12 Model output of the prototype dual-susceptor reactor showing differential pressure in cross section for the simulation of Figure 3-8. The arrows indicate relative gas velocity along the flow channel.

## 1.1 INTRODUCTION

The epitaxial growth of compound semiconductor thin films is crucial to the fabrication of advanced, high speed devices for digital, electro-optic, and mmIC applications. These next generation devices require materials that have atomically sharp heterojunction interfaces. Applications range from high speed HEMT structures for fifth generation supercomputers to quantum and multiquantum well structures for optical communication.

Growth of atomically abrupt heterojunction structures requires tight control over the layer thickness and film uniformity. The necessary control has been achieved by the molecular-beam epitaxial (MBE) technique, but this process is limited by surface defects, throughput capability, and run-to-run reproducibility which may be inadequate for production of the material. Also MBE is not well suited to the deposition of phosphorus-containing compounds, which are becoming increasingly important for optoelectronic devices. These problems have been largely solved by using the OMCVD process, but the OMCVD epitaxial technique still lacks the necessary controls over interface abruptness and, to a lesser extent, layer thickness and uniformity.

Even though vendors of OMCVD equipment have made significant advances in system construction, particularly in the gas manifold design, commercial reaction chambers remain mainly based upon the three basic designs developed for deposition of silicon layers. Silicon deposition is far simpler than deposition of binary, ternary, or quaternary compound semiconductors, and lacks the requirement for the same degree of interface sharpness between layers. There is presently a strong need for the development of an innovative reactor capable of reproducibly depositing uniform layers of compound semiconductors with sharp interfaces to provide material for device production. Large-area deposition is also necessary in order to provide quantities of wafers to fuel the growth of an advanced device industry. The problem addressed in this project may be broadly defined as research on an advanced OMCVD reactor, with emphasis on attainment of large areas of heterostructure layers.

## TECHNICAL APPROACH

As noted above, the two deposition techniques that have the potential to satisfy from production requirements of advanced devices are MBE and OMCVD. The advantage of OMCVD as a production process is its use of a gas flow to achieve large-area deposition at reasonable growth rates. In conventional CVD reactors, it is this same gas flow that is also responsible for spatial variations in the growth rate and lack of abruptness at interfaces. Gases are subject to viscosity effects, convective forces, and depletion effects which all serve to influence the flow and resulting deposition<sup>1</sup>. Thus far existing OMCVD reactors have attempted to control these effects thus far with only limited success.

The ability of MBE to control the deposition process lies in its control over the source delivery. The constituent materials are essentially sprayed in molecular beams out of source vessels into an ultra-high vacuum. The sample is positioned in these beams to intercept the molecules. The molecules therefore arrive at the sample surface with none of the complications present in OMCVD. To obtain a similar level of control at the greater pressures used in OMCVD requires simplification of the gas flow through the reduction or elimination of the various flow effects.

Kopin has developed an innovative design for an OMCVD reactor \* which has a simplified gas flow. This vertical reactor, \* shown schematically in Figure 1-1, uses two distinct disk- \* shaped susceptors that each hold wafers. The susceptors are \* mounted vertically and face one another, creating a \* deposition zone between them. These twin vertical susceptors \* are capable of rotation for enhanced layer uniformity. The \* wafers are mounted rigidly to the susceptor surfaces facing \* the deposition zone. Thus, the deposition zone has twice the \* wafer area and no cold wall facing the wafers as in \* conventional systems. Wafer temperature uniformity is \* improved and, as the susceptors are mounted vertically, the \* wafers' surfaces are not subject to particulate contamination \* during growth. The reactant gases flow vertically upwards \* through the deposition zone in the same direction as the \* buoyant forces created upon heating of the gases. \*

In this Phase I report we will show that the dual-susceptor reactor design is feasible for scale up to larger deposition area. Upward flow of reactant gases has been demonstrated to produce extremely abrupt interfaces in GaAs/AlGaAs layers. We also found that the dual-susceptor reactor was capable of growth at temperatures at 500°C, well below the useful range for conventional reactors. The use of low temperature growth provides additional control over interface and dopant \*

"Use or disclosure of the proposal data on lines specifically identified by asterisk (\*) are subject to the restriction on the cover page of this proposal."



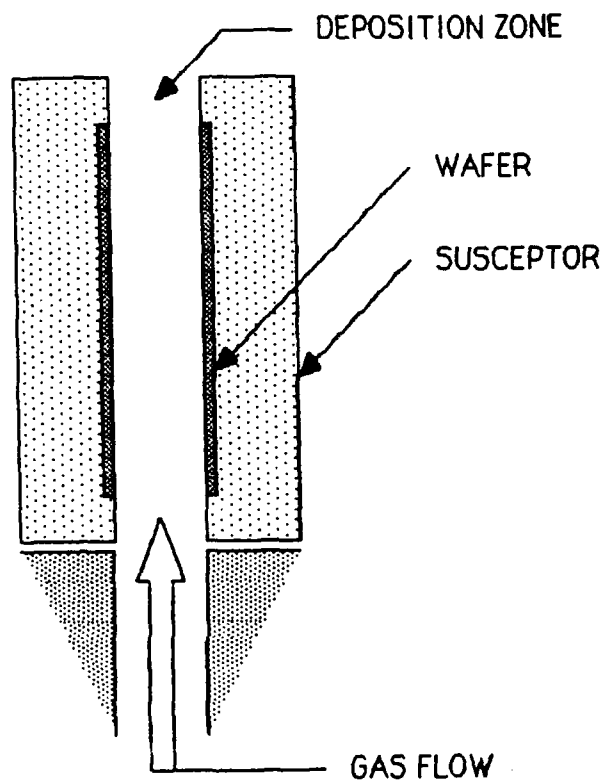


Figure 1-1. Cross sectional schematic of the dual-susceptor reactor.

"Use or disclosure of the proposal data on lines specifically identified by asterisk (\*) are subject to the restriction on the cover page of this proposal."

abruptness in heterostructures. Results of Phase I also \* indicate that this pseudo-hot-wall configuration produces a \* high arsenic pressure in the deposition zone, allowing growth \* at low arsenic to group 3 ratios. Improved arsine \* utilization represents a large advantage for the commercial \* use of such a reactor. \*

## 1.2 DUAL-SUSCEPTOR REACTOR

A prototype reactor was constructed by Kopin to test many aspects of this design. This reactor is shown schematically in Figure 1-2. Each susceptor holds one 2" diameter wafer, \* and is designed to be rotated during deposition. The \* susceptors are raised and lowered into the reactor with a \* stainless steel crane through a gate valve. The susceptors \* may thus be removed from the reactor while still relatively \* hot, shortening both the wafer cooling time and overall \* turnaround time of the growth runs. This reactor was \* interfaced to an OMCVD system for the growth of epitaxial GaAs and AlGaAs layers. The reactor has undergone characterization at Kopin as part of the Phase 1 work. These results are presented in Section 3 of this report. From these studies, a scaled up and improved version of the dual-susceptor will be proposed for Phase II.

## 2.0 PHASE I TECHNICAL OBJECTIVES

The technical objectives of Phase 1 work were as follows:

1. Determine the effect of reactor growth parameters on the uniformity and abruptness of GaAs layers grown in the prototype, first-generation, dual-susceptor OMCVD. These parameters include reactor pressure, gas velocity, and gas inlet configuration.
2. Identify critical design parameters for the scale-up of the dual-susceptor OMCVD. From the results of task 1 above, determine those parameters which could have a significant effect on the uniformity and abruptness of a production dual-susceptor OMCVD.
3. Determine and outline what additional experiments, if any, are necessary to evaluate the above critical design parameters for scale-up.
4. Analyze the dual-susceptor configuration for use in production OMCVD of GaAs/AlGaAs layers.

"Use or disclosure of the proposal data on lines specifically identified by asterisk (\*) are subject to the restriction on the cover page of this proposal."

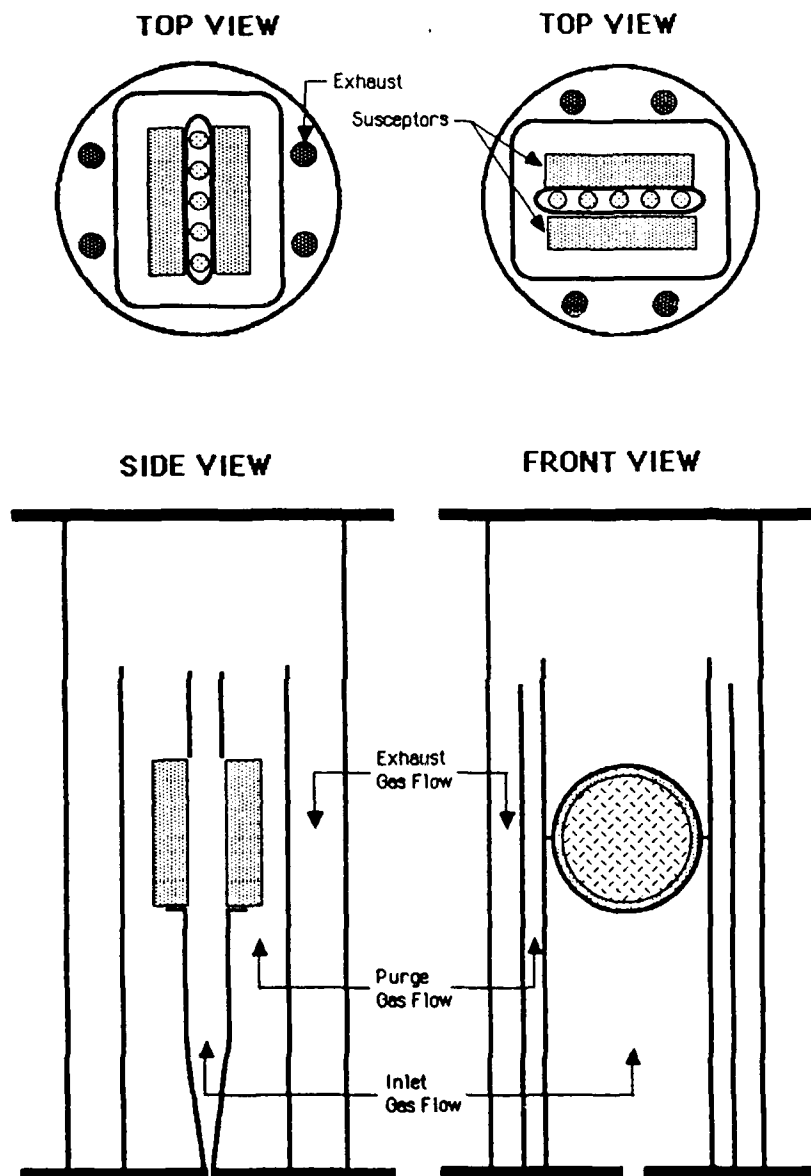


Figure 1-2. Prototype Dual-Susceptor Reactor

"Use or disclosure of the proposal data on lines specifically identified by asterisk (\*) are subject to the restriction on the cover page of this proposal."

### 3.0 SUMMARY OF RESEARCH AND FINDINGS

#### 3.1 Task 1: Growth Parameters

The effect of reactor growth parameters on the uniformity of GaAs layers grown in the prototype dual-susceptor OMCVD was determined. Series of test runs were made in the first-generation reactor while varying reactant gas velocity and reactor deposition pressure. In order to determine growth rate profiles as a function of growth conditions varied, susceptor rotation was not used for these experiments. Growth rates were calculated from growth times and from thickness measurements made in a cross pattern on 2"-diameter wafers.

##### 3.1.1 Reactor Gas Flow

The effect of reactor gas velocity on growth rate uniformity was determined over a range of inlet gas flows. The average reactant gas velocity was calculated by summing the gas flows injected into the reactor and dividing by both the cross sectional area of the deposition zone and the gas pressure in the reactor. The deposition zone cross sectional area for the \* prototype reactor was 7 cm<sup>2</sup>. It should be emphasized that \* the following results were obtained with no susceptor rotation.

Three GaAs deposition runs were made with total gas inject flows of 2.8, 3.7 and 5.5 liters per minute (SLM) at standard temperature and pressure. The reactor pressure and temperature were held constant over these runs at 80 torr and 640°C, respectively. Average gas velocities in the heated deposition zone were calculated for the above three runs at values of 200, 260, and 400 cm/s. The growth rates as a function of vertical position on the wafers for these runs are plotted in Fig. 3-1. The growth rate from all three runs increased in the direction of the gas flow, ie, from the bottom edge of the wafer to the top. This was somewhat surprising as gas depletion effects would cause the growth rate to drop off in the direction of gas flow.[1] Gas depletion effects are diminished under conditions of high flow, however, as the decrease in concentration of the source gas due to diffusion to the substrate becomes negligible at the high flows.

The uniformity of the three runs of Fig. 3-1 was constant with respect to gas flow velocity. This observation is also consistent with high flow conditions and low depletion in the gas. The decrease in the average growth rate as the inject flow was increased was due entirely to the lower source concentration for the runs with higher flow. Since the

"Use or disclosure of the proposal data on lines specifically identified by asterisk (\*) are subject to the restriction on the cover page of this proposal."

trimethylgallium (TMGa) mass flow was held constant for the three runs, the concentration of TMGa in the reactor decreased for runs as the total flow was increased. The TMGa concentration has been reported by numerous workers to control the growth rate of GaAs.[2-4] The average growth rate for the wafers of Fig. 3-1 are plotted in Fig. 3-2 as a function of trimethylgallium concentration. The linear fit of these data points indicates that the growth rate for the stated conditions in this reactor is proportional to the reactor group 3 source concentration.

### 3.1.2 Reactor Pressure

Growth rate uniformity was also measured on wafers from a series of deposition runs with different reactor pressure and at two deposition temperatures. In one series of runs the inject gas flow and temperature were held constant at 3.7 LPM and 580°C, respectively. Three deposition pressures of 80, 120, and 240 torr were used. The reactor pressure was controlled by a throttle valve and electronic controller with pressure measured by a baratron. The growth rate along the vertical center section of these wafers is plotted in Fig. 3-3. Increases in the deposition pressure from 80 to 120 and 240 torr resulted in several key changes. First, the uniformity of the wafers along the direction of the gas flow improved from a range of  $\pm 7\%$  to ranges of  $\pm 4\%$  and  $\pm 2\%$  for growth at 120 and 240 torr. Second, the uniformity profile changed from higher growth rates at the top of the wafer to higher growth rates occurring near the bottom of the wafer. This result indicates that the deposition pressure in this reactor was critical for growth rate uniformity and, by careful choice of pressure, the uniformity may be optimized further. The optimum uniformity for a growth temperature of 640°C appears to be obtained at a pressure between 80 and 120 torr.

The observed profile for the deposition pressure of 240 torr is indicative of source depletion in the carrier gas. As the pressure is increased, the velocity of the gas in the deposition zone decreases a proportional amount. Thus, the gas velocity at 240 torr is half of that at 120 torr and one-third the velocity at 80 torr. The lower velocities allow greater source depletion as the gas passes by the wafer, which results in larger growth rates where the gas initially deposits on the wafer. The change in growth rate is somewhat offset by lower source diffusivities at the higher pressures. The relative contributions of these effects will be modelled in Phase II of this work.

Even greater reactor deposition pressures were used in a series of runs made at 580°C. Fig. 3-4 shows the growth rate

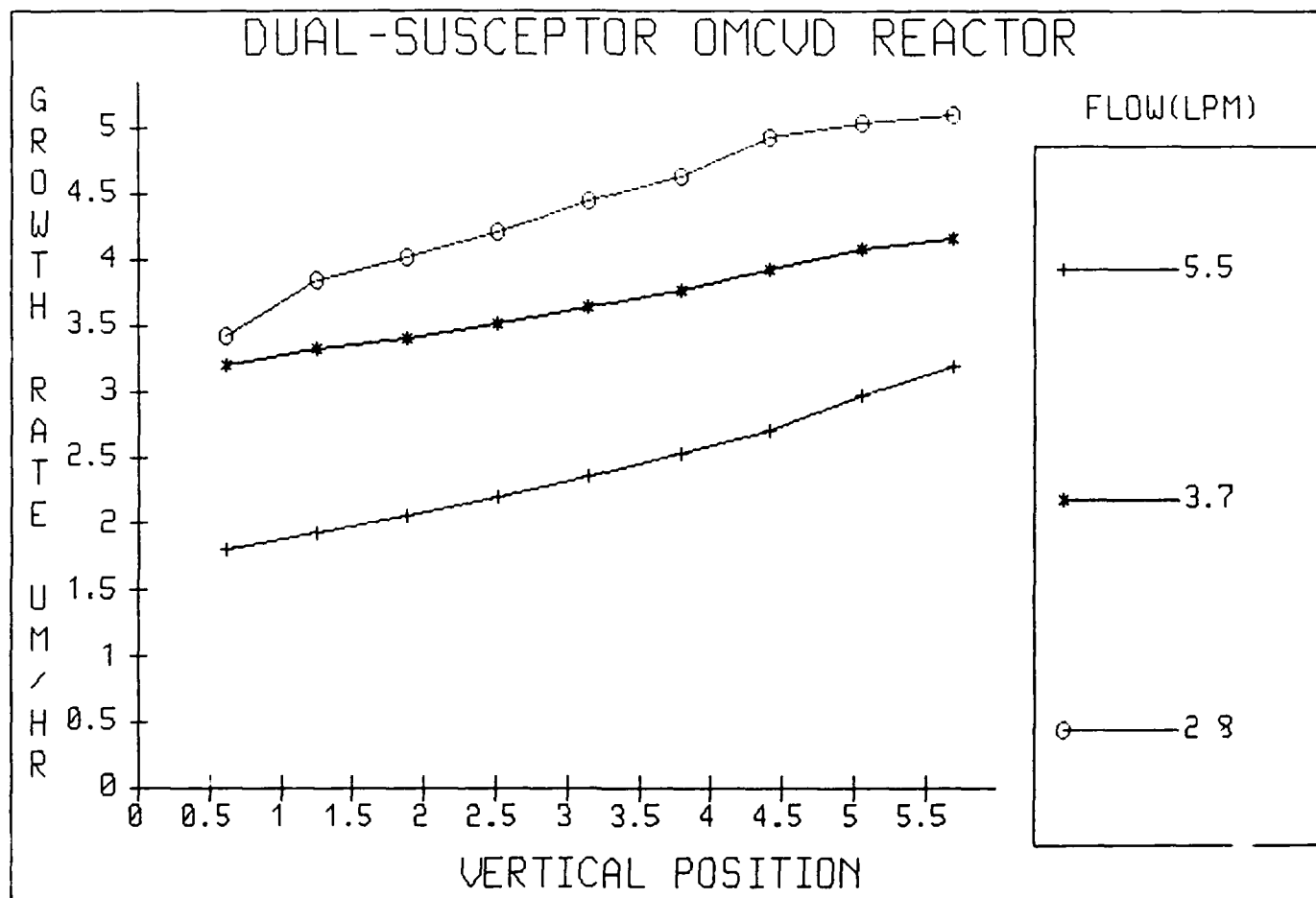


Figure 3-1 Growth rate plotted as a function of vertical position along a 2" wafer for deposition at three different gas flow rates.

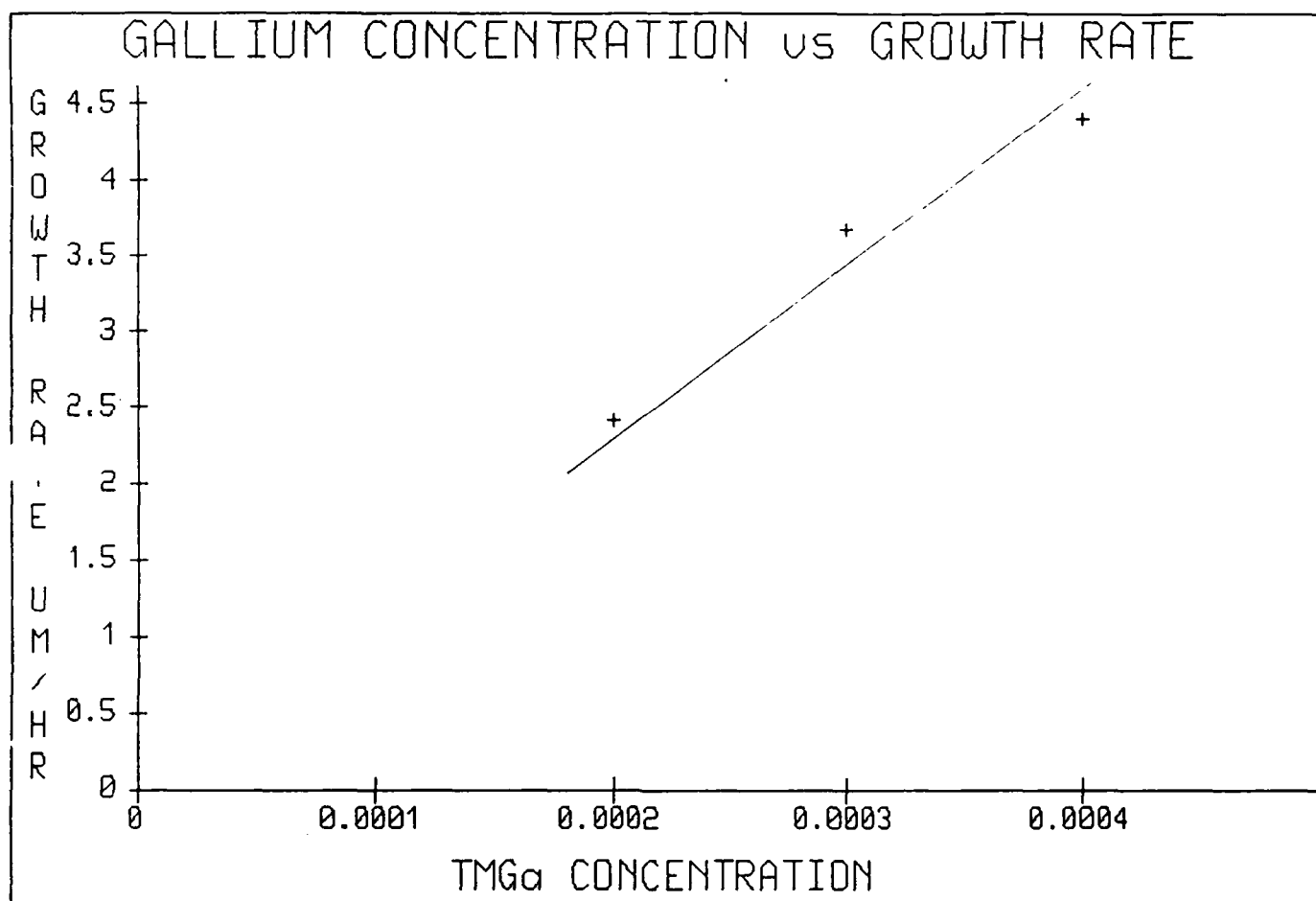


Figure 3-2 Average growth rate

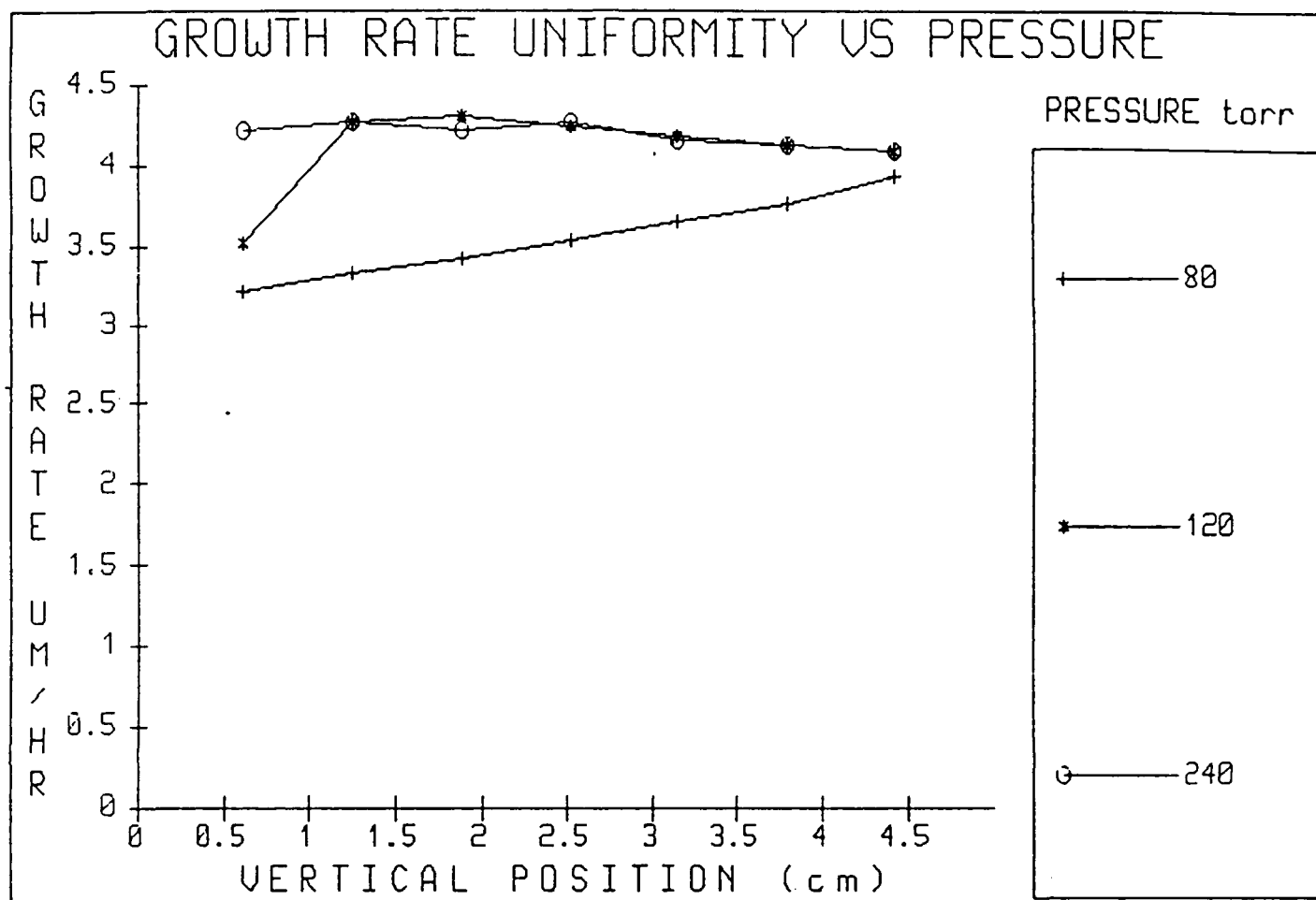


Figure 3-3 Growth rate uniformity along 2" wafers deposited at a temperature of 640°C and pressures of 80, 120, and 240 torr.



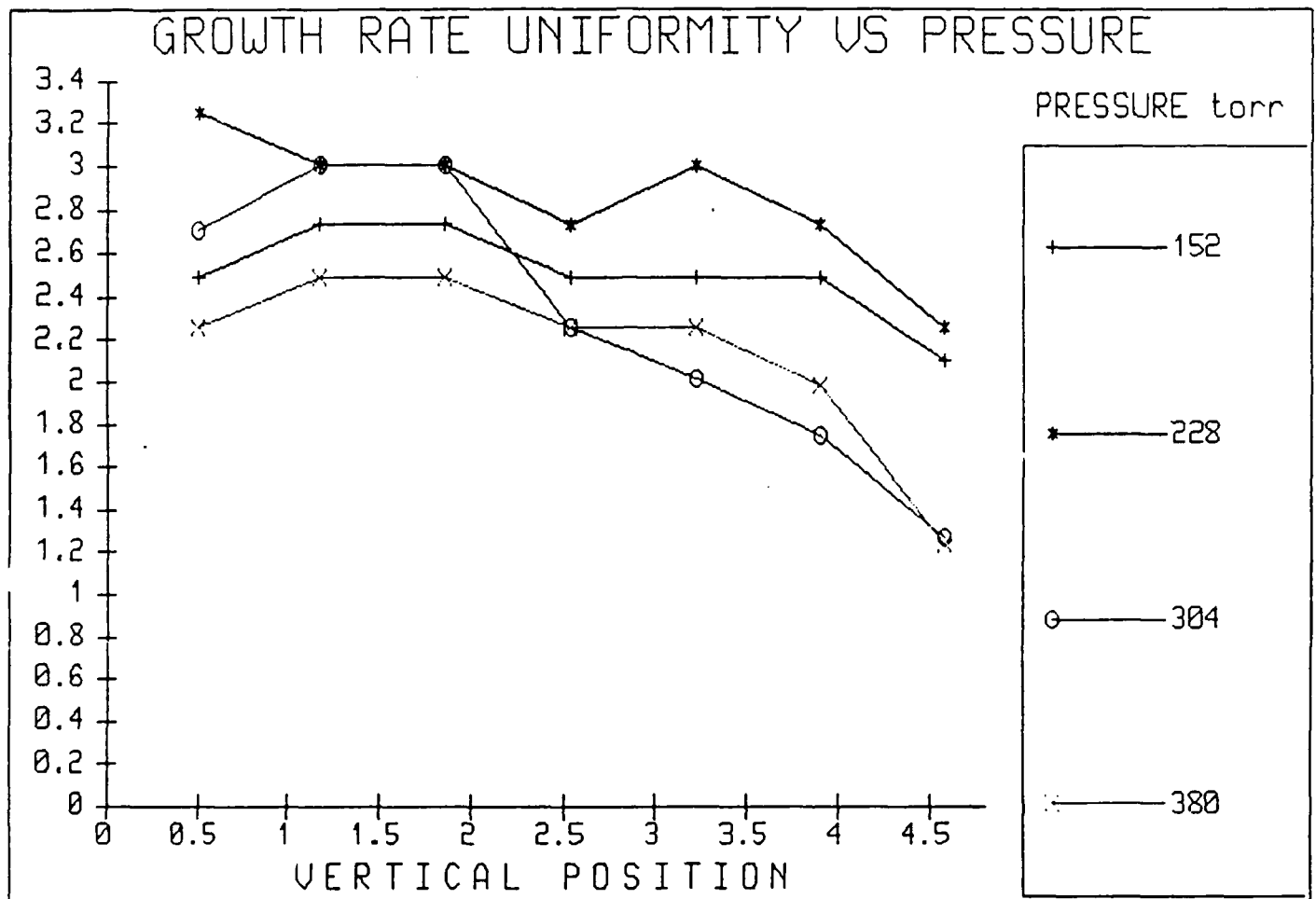


Figure 3-4 Growth rate uniformity along 2" wafers deposited at a temperature of 580°C and 152, 228, 304, and 380 torr.

along the center vertical section of wafers deposited at pressures of 152, 228, 304, and 380 torr. The shapes of the curves are the same as those corresponding to similar pressures in Fig. 3-3, although the uniformity apparently worsened as the pressure was increased past 228 torr to 304 torr. The optimum uniformity for this temperature appears to be obtained at a pressure less than 152 torr.

The above results are very significant to uniformity in this reactor. By adjusting the reactor pressure, the growth rate profile along the wafer can be changed from a positive slope to a negative slope. Therefore, the uniformity can be optimized based upon the reactor pressure, an easily controlled parameter. The results also indicate that susceptor rotation may not be needed. However, optimized uniformity coupled with rotation should lead to extremely uniform layers which may equal or surpass those grown by MBE.

### 3.1.3 Gas Inlet Configuration

The above discussion has been involved only with the growth rate on the wafer along the direction of the gas flow, or the vertical. The growth rate on the wafer in a section normal the gas flow, or horizontally, was also measured on some wafers. The horizontal uniformity is dependent primarily on the distribution of gas from one side of the wafer to the other. This gas distribution is in turn a function of the gas inlet configuration, or the manner in which the gas is injected into the base of the reactor flow channel.

The gas inlet configuration in the first-generation reactor \* consisted simply of a hole, 0.175" in diameter, in the middle \* of the reactor base plate. This configuration is shown in \* Fig. 3-5. Allowance was made just above the hole to insert a \* diffuser plate to laterally distribute the inlet gas. Once \* the reactor had been operating, removal of the flow channel \* to insert a plate proved to be too difficult as the o-ring at \* the channel base was tight against the channel. The attempt \* was postponed due to lack of a replacement flow channel. \*

An example of the lateral uniformity obtained with the above gas inlet configuration is shown in Fig. 3-6. The wafer was deposited at 640°C and 120 torr with a total gas flow of 3.7 LPM. The lateral range of growth rate is  $\pm 17\%$ , as compared to a vertical range of  $\pm 4\%$  on this wafer. The large difference in deposition rate between one side and the other indicates that the flow was not symmetric across the deposition zone. This lateral nonuniformity was independent of growth pressure and total gas flow.

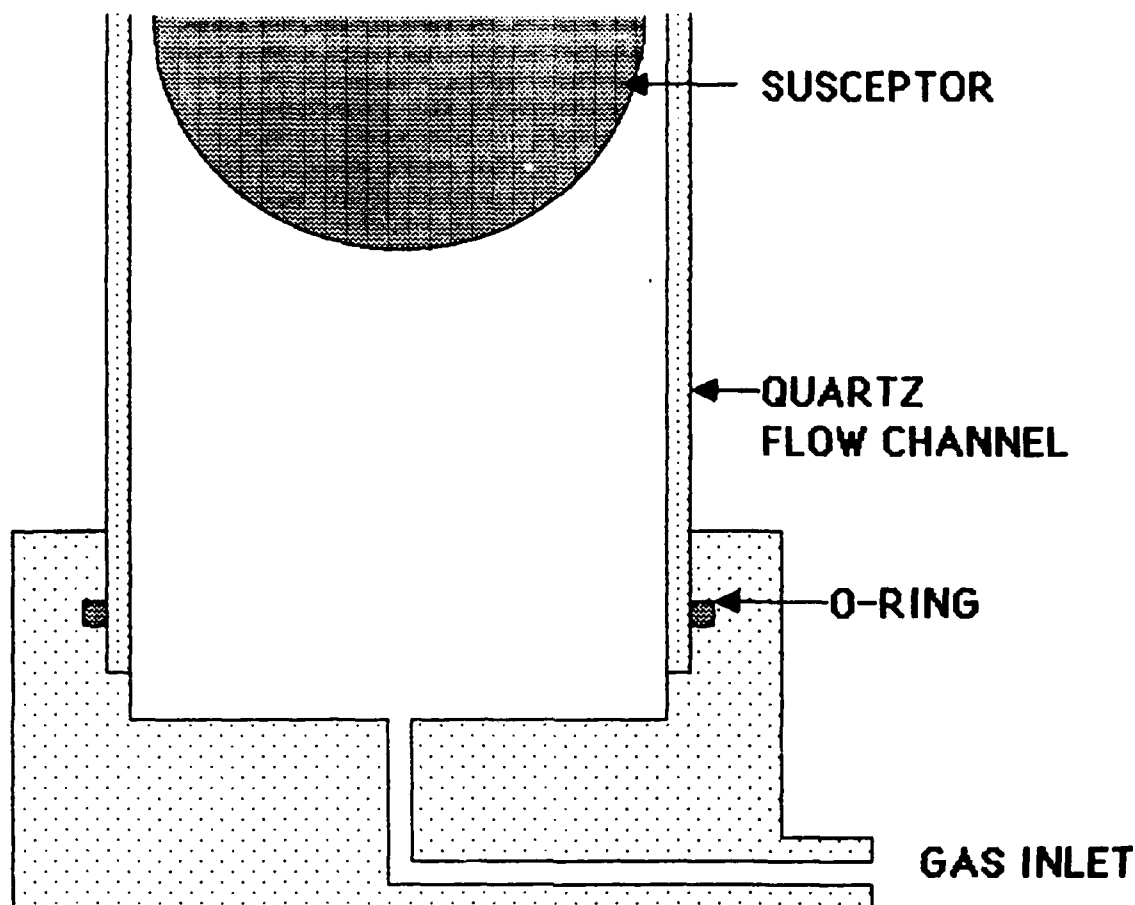


Figure 3-5 Gas inlet configuration in the prototype reactor.

"Use or disclosure of the proposal data on lines specifically identified by asterisk (\*) are subject to the restriction on the cover page of this proposal."

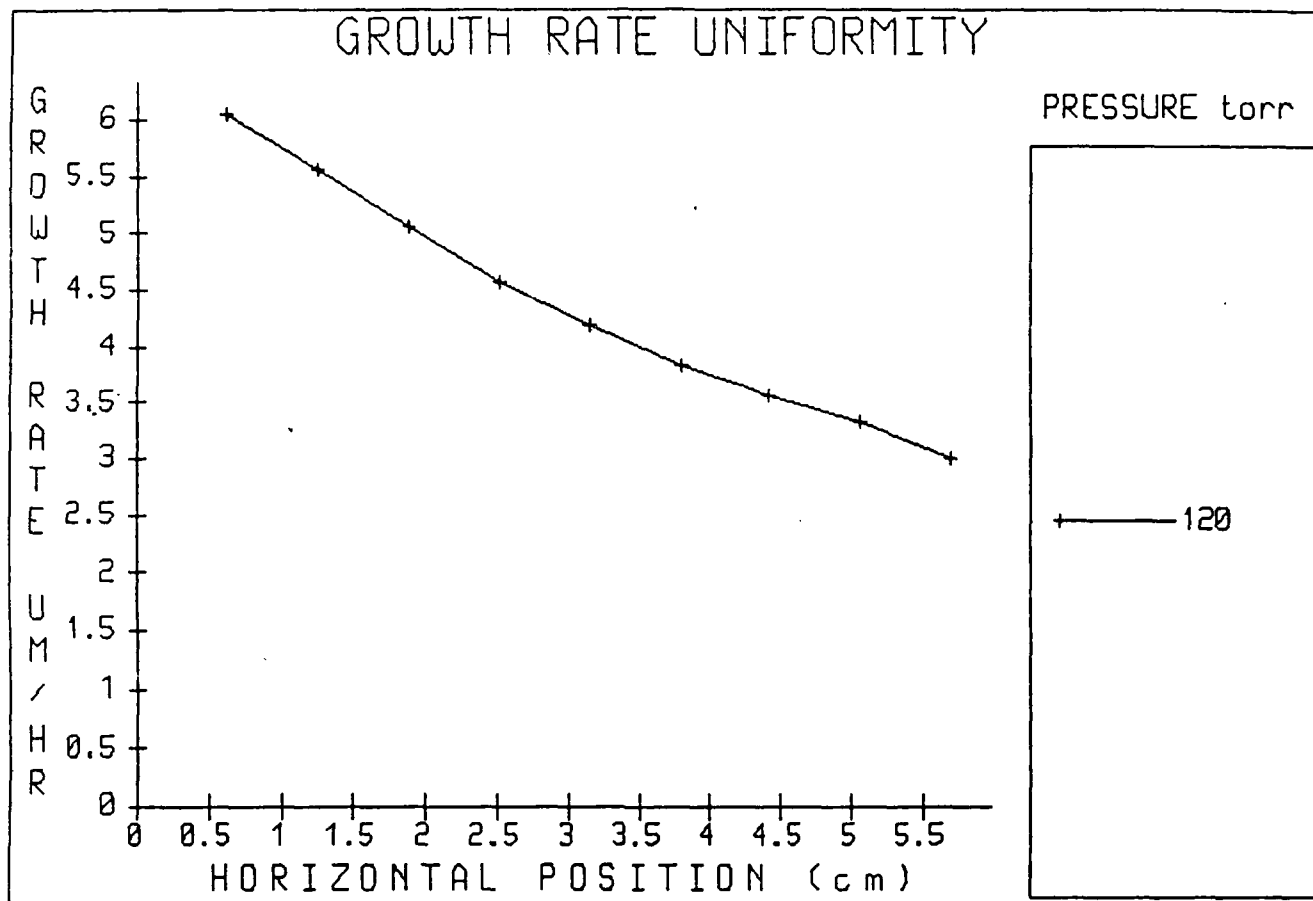


Figure 3-6 Lateral growth rate uniformity of a wafer deposited at 640°C and 120 torr.



Figure 3-7 Cross sectional transmission electron micrograph of a GaAs/AlAs heterostructure.

The inlet flow configuration must be studied further, and allowance must be made in the scaled up dual-susceptor reactor for fitting changes at the reactor inlet. The inlet configuration has therefore been designated a critical design parameter for the scale up.

#### 3.1.4 Interface Abruptness

In order to demonstrate the abruptness of the first generation reactor, a multilayered structure of GaAs and AlAs was deposited, and a portion of the wafer was prepared in cross section for transmission electron microscopy (TEM). Figure 3-7 is an enlargement of a TEM micrograph of that sample. The light areas correspond to AlAs layers, and the darker areas to GaAs layers. The substrate is denoted by "SU" on the lower left corner of the micrograph. The shortest growth duration used for the AlAs layers was 10 seconds, and resulted in layer thicknesses of about 7.5 nm. There were no interruptions in growth between the layers. The sharpness of the interfaces confirms that this reactor design can deposit abrupt, thin layers.

Extensive experimentation on the abruptness in this reactor was cut short by the breakage of the flow channel. This quartz piece was custom fabricated and a replacement could not easily be obtained. The first-generation reactor was therefore gracefully retired in favor of working towards an improved, larger model. Two lessons were emphasized by this reactor's demise: minimize the number and complexity of quartz reactor parts, and allow for quick and easy replacement of those quartz parts which must be used.

### 3.1.5 Chemical Utilization

The chemical utilization for both group 3 and group 5 compounds was investigated in the first-generation dual-susceptor reactor. Utilization of the group 3 compound, trimethylgallium (TMGa), was calculated from the average growth rate, the flux of TMGa into the reactor, and the total wafer deposition area. The runs corresponding to Figs. 3-1 and 3-2 exhibited TMGa utilization of about 20%, which was typical for most of the conditions studied. Even greater utilization of TMGa may be achieved, but at the expense of growth rate uniformity.

Arsine utilization was calculated in a similar manner to TMGa utilization. Because of the high vapor pressure of arsenic at growth temperatures, GaAs is typically deposited in conversational low pressure reactors with Group 5 to Group 3 ratios from 20 to several hundred in order to maintain arsenic pressures at the GaAs surface and prevent the surface from deteriorating. The typical 5/3 ratio used in this work was 30, leading to an arsine utilization of slightly less than 1%. A series of runs was made at 580°C and 50 torr with several lower 5/3 ratios, and the surfaces of the wafers subsequently inspected. Layers deposited even at the lowest ratio of 7.5 exhibited smooth surfaces, indicating sufficient arsenic pressure and excellent arsine cracking during growth. Arsine utilization for this particular run was 3%. The lowest ratio used was limited only by the range of the mass flow controllers in the OMCVD system. The two hot walls of the deposition zone prevents the arsenic from condensing and apparently keeps more of it available for growth along the entire susceptor. We believe that high-quality growth with 5/3 ratios as low as 1 are possible with the dual-susceptor reactor, with corresponding arsine utilization efficiencies of 20%.

### 3.1.6 Low Temperature Growth

The efficient utilization of arsine in the first generation reactor allowed growth of GaAs with high surface quality at temperatures as low as 500°C. A series of runs were made at growth temperatures in the range of 580 to 480°C, with a reactor pressure of 50 torr, a total gas flow of 3.7 LPM, and a 5/3 ratio of 30. The GaAs surfaces were specular for runs made at temperatures down to 500°C. GaAs grown at 480°C though, had surfaces which exhibited features with an approximate density of  $3 \times 10^5/\text{cm}^2$  denoting Ga droplets. The GaAs growth rate was between 3 and 4  $\mu/\text{hr}$  for all the wafers grown in this series of runs, and did not exhibit temperature dependence. This result indicates a significant arsenic vapor pressure in the deposition zone even at these low

temperatures. There are two probable causes for this effect. As pointed out in the previous section, the hot susceptors prevent excess arsenic condensation in the deposition zone. Second, the pseudo-hot wall configuration heats the gas more efficiently, causing more efficient decomposition of the arsine source gas. This latter effect is discussed in more detail in a following section on additional experiments.

### 3.2 Task 2: Critical Design Parameters

From the above results, it is clear that reactor pressure is a critical design parameter. Pressure control in the range of 50 to 300 torr is required, and reproducibility of pressure setpoint is necessary for control over the wafer uniformity in the direction of gas flow. \*

Growth rate uniformity laterally across the wafer was largely unaffected by changes in the growth conditions investigated. We believed that the gas inlet flow configuration controlled the lateral uniformity, but were unable to experiment with the inlet on the prototype reactor. The gas inlet configuration is the means of dispersing the gas as it enters the lower end of the reactor, and therefore should determine the actual gas flow distribution in the reactor. Since the deposition zone is narrow between the susceptors, the gas distribution of interest for uniformity is primarily in the lateral dimension. \*

The inlet flow configuration must be studied further, and allowance must be made in the scaled up dual-susceptor reactor for fitting changes at the reactor inlet. The inlet configuration has therefore been designated a critical design parameter for the scale up. \*

Operational issues, such as susceptor removal and insertion, were also evaluated in the prototype reactor. Movement of the susceptors was found to be both reliable and reproducible, and did not appear to cause particle contamination of the substrates. Using a laser scanning surface mapping system, layers were grown with as few as 4 surface defects per  $\text{cm}^2$  greater than  $2\mu\text{m}^2$  in area. This surface quality of wafers after deposition in the prototype was equal to or superior to that of wafers deposited in Kopin's other deposition systems. \*

Another operational issue was reactor maintenance. Although the prototype was not designed for extended use, its components were designed for removal and cleaning. In practice, we found that the o-ring seal used on the central flow channel would not allow easy removal of this piece. Not \*

"Use or disclosure of the proposal data on lines specifically identified by asterisk (\*) are subject to the restriction on the cover page of this proposal."



being able to remove this central piece of quartz, the two \*  
susceptor rotation mechanisms were difficult to access and \*  
repair when the drive wires broke. These problems did not \*  
prevent use of the reactor until the flow channel started to \*  
crack, but they clearly pointed out the need for both \*  
reliable components and access to the different subassemblies \*  
in the reactor chamber. Quartz components should be simple \*  
to fabricate and few in number. Susceptor rotation should be \*  
direct drive. The flow channel and inlet fitting must be \*  
easily removable for cleaning or modification. \*

The heating system for the prototype reactor consisted of an \*  
RF generator controlled by a thermocouple and temperature \*  
controller. The thermocouple was in contact with one of the \*  
susceptors, which were inductively heated by the RF coil \*  
outside the reactor. Although this system worked, it had \*  
several drawbacks. First, the thermocouple could not have \*  
adequately monitored the temperature of the susceptor had it \*  
been rotating. Second, the use of RF heating required \*  
materials around the susceptors to be nonconducting, \*  
including the quartz outer wall of the reactor. The system \*  
could be improved by using an infrared pyrometer for the \*  
temperature measurement. For scaling up to larger susceptor \*  
diameters, the RF would have to be located inside the \*  
chamber, close to each susceptor. Alternative heating \*  
sources need to be evaluated. \*

To summarize the critical design parameters for the scale up \*  
of the dual-susceptor reactor are reactor pressure and inlet \*  
gas configuration. Operational issues which warrant further \*  
attention include ease of maintenance, susceptor rotation, \*  
and susceptor heating. \*

### 3.3 Task 3: Additional Experiments \*

Additional experiments are necessary in Phase II to evaluate \*  
the inlet gas configuration. To obtain the best uniformity \*  
in the scaled up reactor, the inlet gas should be made to \*  
pass through a fitting or fixture which distributes the gas \*  
in an appropriate manner. The optimum fitting will need to \*  
be determined empirically, and therefore the reactor would \*  
have to be designed with the ability to easily change the \*  
inlet fitting. \*

In order to help manage the risk associated with scale-up, \*  
work was carried out to install and run an OMCVD growth \*  
model. The model is a simulation using finite difference \*  
treatment of the physical processes which occur in the gas in \*  
an OMCVD reactor. The physical processes are introduced \*  
through four conservation equations: mass, source species, \*  
energy, and momentum. It calculates gas temperature, gas \*

"Use or disclosure of the proposal data on lines specifically identified by  
asterisk (\*) are subject to the restriction on the cover page of this  
proposal."

velocities, pressure, concentration of the reactants, and growth rates and uniformity along the wafer. There are three approximations and two assumptions in the model:

1. All heat sources originating in the gas are neglected.
2. Gas phase reactions are neglected.
3. Thermal diffusion is neglected.
4. The model is two dimensional; flow in the third dimension is assumed to be zero.
5. The gas inlet distribution is assumed to be either parabolic or flat.

The three approximations are appropriate for the growth of AlGaAs. The two assumptions are reasonable but need to be experimentally verified.

Initial testing of the model indicates agreement with experimental results for some of the growth conditions tested. Its application for other conditions is limited by the potential presence of flow in the third dimension. In general, the experimental results indicated better uniformity than the model. For example, the deposition run corresponding to the curve for 228 torr pressure in Fig. 3-4 was simulated, and the results plotted in Fig. 3-8 along with the experimental curve. The agreement in the upper half of the wafer is very good, while the model predicts a greater growth rate for the lower portion of the wafer. The difference may be due to inaccuracies in the physical constants initially being used in the model, and needs to be investigated further.

The shape of the above curves can be seen to derive from source gas depletion shown in Figure 3-9, a cross sectional map of the flow channel and deposition zone. The scale covers TMGa mass fraction from 0.0 to 1.0 in ten steps with full scale corresponding to a concentration of 0.0003. The modelled TMGa mass fraction dropped off in the deposition zone to less than 0.2 of its starting value, providing less source gas for growth at the top of the susceptors than at the bottom. The lower TMGa concentration is somewhat offset by the higher gas velocities produced as the gas is heated through the deposition zone. Figure 3-10 is another map from the model showing vertical gas velocity for the same simulation as in Figs. 3-8 and 3-9. The scale is from 0 to 80 cm/s for the simulated pressure of 228 torr. The velocity first decreases as it expands coming out of the inlet at the

"Use or disclosure of the proposal data on lines specifically identified by asterisk (\*) are subject to the restriction on the cover page of this proposal."

# MASS FRACTION

Full Scale =

1.455E-02

1.000

0.900

0.900

0.800

0.800

0.700

0.700

0.600

0.600

0.500

0.500

0.400

0.400

0.300

0.300

0.200

0.200

0.100

0.100

0.000

DUAL-SUSCEPTOR OMCUD Run #5154 Simulation

1.64 0.82 0.00

9.10 9.10

4.03

4.03

-1.1

-1.0

-6.1

-6.1

-11.

-11.

1.64 0.82 0.00

Figure 3-9 Model output of the prototype dual-susceptor reactor showing TMGa mass fraction in cross section for the simulation of Figure 3-8

\* " Use or disclosure of the proposal data on lines specifically identified by asterisk (\*) are subject to the restriction on the cover page of this proposal."

AXIAL VELOCITY UX:

DUAL-SUSCEPTOR OMCVD Run #5154 Simulation

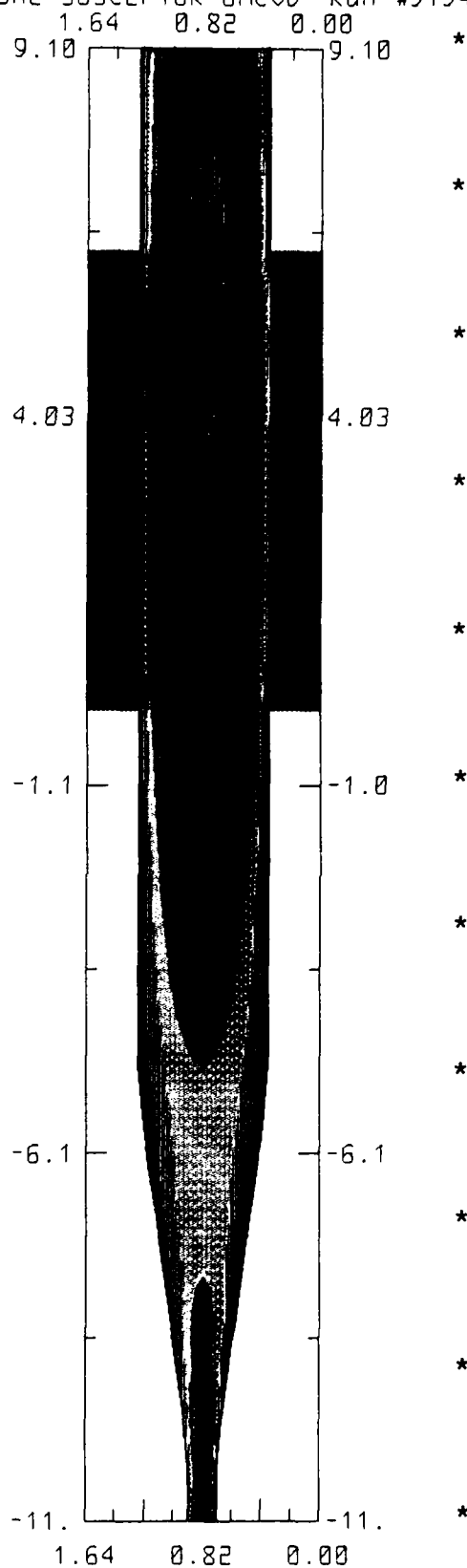
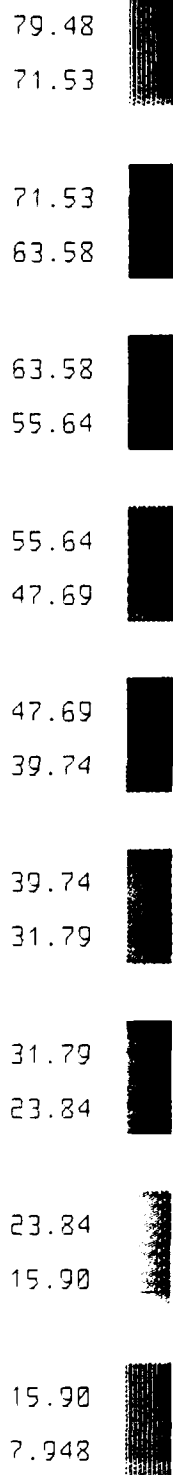


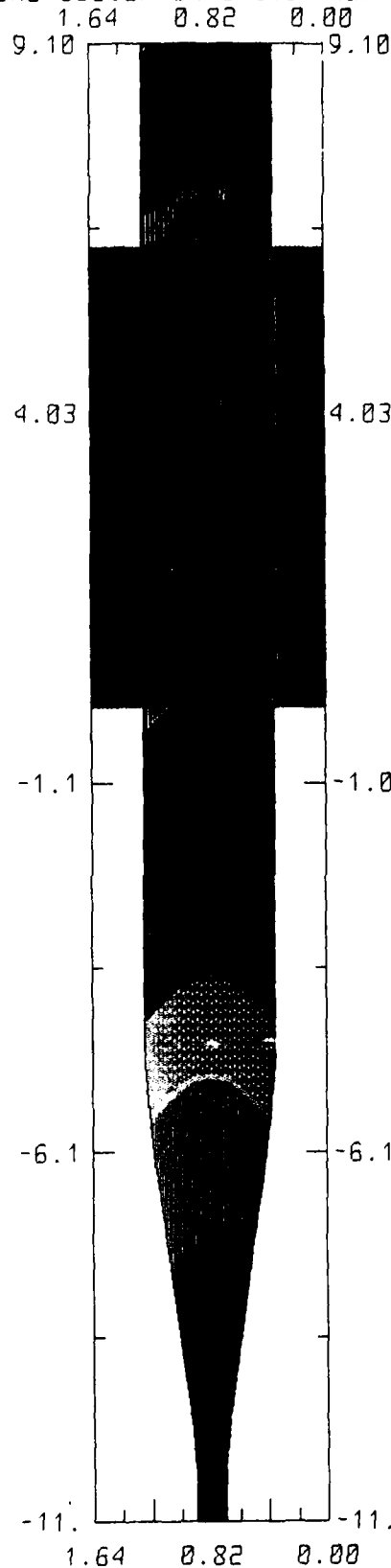
Figure 3-10 Model output of the prototype dual-susceptor reactors showing temperature in cross section for the simulation of Figure 3-8.

\* "Use or disclosure of the proposal data on lines specifically identified by asterisk (\*) are subject to the restriction on the cover page of this propo

TEMPERATURE MAP:

DUAL-SUSCEPTOR OMCUD Run #5154 Simulation

853.0  
797.7  
  
797.7  
742.4  
  
742.4  
687.1  
  
687.1  
631.8  
  
631.8  
576.5  
  
576.5  
521.2  
  
521.2  
465.9  
  
465.9  
410.6  
  
410.6  
355.3



355.3  
300.0

Figure 3-11 Model output of the prototype dual-susceptor reactor showing vertical velocity of the gas in cross section for the simulation of Figure 3-8.

\* "Use or disclosure of the proposal data on lines specifically identified by asterisk (\*) are subject to the restriction on the cover page of this proposal."

ADDED PRESS dyne/cm2

Full Scale =

1.068E+00

0.031

-0.07

-0.07

-0.18

-0.18

-0.28

-0.28

-0.38

-0.38

-0.48

-0.48

-0.59

-0.59

-0.69

-0.69

-0.79

-0.79

-0.90

-0.90

-1.00

DUAL-SUSCEPTOR OMCVD Run #5154 Simulation

1.64 0.82 0.00

9.10 9.10

4.03

4.03

-1.1

-1.0

-6.1

-6.1

-11.

-11.

1.64 0.82 0.00

Figure 3-12 Model output of the prototype dual-susceptor reactor showing differential pressure in cross section for the simulation of Fig 3-8. The arrows indicate relative gas velocity along the flow channel.

\* "Use or disclosure of the proposal data on lines specifically identified by asterisk (\*) are subject to therestriction on the cover page of this propo

bottom of the reactor, and then increases as it is heated by the susceptors. The maximum velocities occur at the top of the deposition zone. \*

The corresponding temperature map is shown in Figure 3-11. The gas begins to be heated several inches before reaching the deposition zone, attaining a temperature uniform to within 50°C while between the two susceptors. It is this hot deposition zone which allows the reactor to efficiently use the source chemicals and, in the case of the arsine, to crack it and also use the excess arsenic. In addition, there is no large thermal gradient near the susceptors, indicating that the reactor is capable of exceptional thermal uniformity. \*

Figure 3-12 is a map of the differential pressure for the above simulation, showing level isobars in the gas flow. Superimposed on pressure are arrows corresponding to the relative gas velocities in the flow channel. These arrows show parabolic flow up the channel, with no indication of horizontal flow components in the gas. This thermally stable, unidirectional flow provides the basis of control for the dual-susceptor reactor design. \*

#### 3.4 Task 4: Scale Up Analysis \*

The reactor operation was analyzed with respect to the following operational parameters: wafer throughput, loading and unloading operation, maintenance, cleaning, heating and cooling cycles, source usage, and cost of operation. Problem areas in the reactor operation were identified and, in Phase II, will be used as input to the overall scale up reactor design. \*

Wafer throughput is limited in most OMCVD systems by the actual growth time, reactor capacity, loading and unloading operations, and heating and cooling of the wafers. The growth rates in the dual-susceptor reactor were adjustable over the normal range for other OMCVD reactors, from 1 to 6  $\mu\text{m}/\text{hour}$ . The dual-susceptor reactor capacity is potentially very large for several reasons. First, there are two susceptors with wafers, doubling the throughput of a similarly sized pancake or horizontal reactor. Second, as the reactor is scaled up, the flow channel size and the gas usage only scale linearly and not as the square of the susceptor diameter. \*

Loading and unloading of the dual-susceptor were each achieved in two steps. In one step the wafers were placed into the susceptors outside the reactor. As we had spare susceptors for the first-generation reactor, this step was \*

"Use or disclosure of the proposal data on lines specifically identified by asterisk (\*) are subject to the restriction on the cover page of this proposal."

carried out independent of reactor time and therefore did not add any time in the throughput calculation. The second step was the loading and unloading of the susceptors into and out of the reactor. This step was accomplished by a pair of robotic arms in less than one minute. A scaled up reactor would take a similar amount of time. Removal of the susceptors while still hot was made possible by the robotic crane. Susceptors were removed from the reactor at temperatures of 100°C, and allowed to cool to room temperature outside of the reactor in the glovebox. This procedure should be used in a scaled up reactor to remove susceptors at even higher temperatures to a cooling station and eliminate a portion of time in the cooling cycle.

Experience on maintenance and cleaning gained from the first-generation reactor pointed out the need for ready access to the reactor interior. This was achieved with the load-gate valve, through which the interior of reactor was vacuumed out. As the susceptors are removed from the reactor after each run, susceptor cleaning and maintenance is transparent to the reactor operation. However, as previously pointed out, better access to the rotation mechanisms and the gas inject fixture must be designed into the reactor.

Source utilization was demonstrated to be efficient in the first generation dual-susceptor reactor. It is expected that source usage in a scaled up version would remain the same. In addition, the limits of efficiency were not reached in experiments performed in the Phase I work, and even higher source utilization efficiencies are expected upon scale up.

With high capacity, high throughput, and high source utilization, the dual-susceptor reactor has low cost per deposition run. The overall cost of operation in this case will be determined by the process yield. The cost of six 3"-diameter GaAs substrates is approximately \$1,400, over an order of magnitude larger than the cost of source material used in a run. Therefore, low cost of operation will only ultimately be achieved with the reliable and reproducible operation of the reactor.

"Use or disclosure of the proposal data on lines specifically identified by asterisk (\*) are subject to the restriction on the cover page of this proposal."



#### 4.0 REVIEW OF OBJECTIVES

Progress on the original objectives of the Phase I work is summarized below by task.

##### 4.1 Growth Parameters.

The effect of reactor pressure and gas velocity on the uniformity of GaAs layers grown in the prototype dual-susceptor OMCVD was determined. Doping experiments on the reaction time of the prototype reactor were carried out and indicate that the reactor can deposit doped layers in times less than five seconds.

##### 4.2 Design Parameters.

Reactor pressure and inlet gas configuration were identified as critical design parameters for the scale-up of the dual-susceptor OMCVD. The reactor pressure provided excellent control over vertical uniformity while the inlet gas configuration was found to dominate lateral uniformity. In addition, operational issues which warrant further attention include ease of maintenance, susceptor rotation, and susceptor heating. \*

##### 4.3 Additional Experiments.

Additional experiments were found to be necessary for the gas inlet configuration. These should be carried out in the scaled up reactor. A model was brought up which will be used in Phase II to simulate the larger reactor in order to help determine the reactor geometry. Time-dependent analysis needs to be debugged on the model to also allow simulations of interface deposition. \*

##### 4.4 Scale Up Analysis.

The dual-susceptor configuration was analyzed for use in production OMCVD of GaAs/AlGaAs layers. The critical design parameters and important operating issues were identified using the small first-generation reactor.

"Use or disclosure of the proposal data on lines specifically identified by asterisk (\*) are subject to the restriction on the cover page of this proposal."

## 5.0 ANALYSIS OF FEASIBILITY

We believe that the many features of a scaled up dual-susceptor reactor have been demonstrated or have been shown to be feasible. The technological feasibility of each feature is estimated below in order of estimated importance to the final objective of producing a production dual-susceptor reactor. Probably the most significant step remaining is to integrate the features and capabilities of the approach into a workable design.

**UNIFORMITY:** Control over uniformity was demonstrated in the prototype reactor.

**INTERFACE ABRUPTNESS:** Rapid dopant switching was exhibited by the prototype. Atomically abrupt interfaces were previously shown to be achievable in a reactor with a similar upward gas flow.

**LARGE AREA:** By using a growth model to simulate a scaled up version of the reactor, we believe we can achieve excellent uniformity and abruptness over six 3"- or even 4"-diameter wafers per run.

**EFFICIENT CHEMICAL UTILIZATION:** Efficient utilization of source chemicals was shown, particularly of the group 5 source. Source chemical usage in a scaled up reactor will be manageable.

## 6.0 SUMMARY

In summary, experiments on a first-generation dual-susceptor reactor show that the reactor design has the potential for scale up to a large-area production reactor capable of the growth of extremely uniform and abrupt layers. Uniformity can be controlled by growth conditions and inlet configuration. Abruptness is inherent in the design of the stable gas flow. The risk of scaling up the design is minimized by the use of a growth simulation model. Efficient utilization of the source gases was demonstrated. Therefore, we find the proposed approach to layer production to be feasible.

REFERENCES:

1. H. Moffat and K. F. Jensen, J. Crys. Growth 77 (1986) p. 108.
2. H. M. Manasevit and W. I. Simpson, J. Electrochem. Soc. 116 (1969) p. 1968.
3. M. R. Leys and H. Veenvliet, J. Crys. Growth 55 (1981) p. 145.
4. H. Krautle, H. Roehle, A. Escobasa, and H. Beneking, J. Electron. Mater. 12 (1983) p. 215.